Biophysical Characterization of the Interaction of the β-Lactamase TEM-1 with Its Protein Inhibitor BLIP†

Shira Albeck and Gideon Schreiber*

Department of Biological Chemistry, The Weizmann Institute of Science, Rehovot, 76100 Israel

Received July 22, 1998; Revised Manuscript Received October 5, 1998

ABSTRACT: BLIP is a secreted protein from *Streptomyces clavuligerus* that inhibits a wide range of β-lactamases. Here we investigate the tight interaction of BLIP, expressed heterologously in *E. coli*, with TEM-1. Kinetic and thermodynamic constants were determined using methods with the proteins either in a homogeneous or in a heterogeneous phase. While values of $\Delta\Delta G_{(mut-wt)}$ are similar whether measured by fluorescence quench, enzyme inhibition, or surface plasmon resonance, absolute values of ΔG and kinetic constants vary. Association and dissociation rate constants of 10^5 M^{-1} s^{-1} and 10^{-4} s^{-1}, respectively, and a nanomolar affinity were determined for the wild-type proteins. The highest affinity is measured at pH 7.5, with a decreasing association rate constant at higher pH values, and an increasing dissociation rate constant at lower pH values. The marginal effect of salt on the kinetics of binding, as well as the calculated surface potentials, suggests a limited role for electrostatic forces in guiding this reaction. Still, mutations of interfacial residues affect the rate of association significantly, so that an increase in the net negative charge on either protein reduces the association rate constant. We show that simple electrostatic rules can explain this behavior. BLIP inhibits the catalytic activity of TEM-1 by binding its active site. Yet, mutations of active site residues on TEM-1 only have a moderate though cooperative effect on the binding energy. This can be explained in light of the peripheral location of the active site in the interface between the two proteins.

Increasing numbers of high-resolution crystallographic studies of protein−protein interfaces have emerged in the past decade. However, structural analysis alone cannot predict which interactions are energetically important for tight binding nor the mechanism by which protein docking occurs. Structural parameters such as buried surface area, the number of van der Waals contacts made by each side chain, crystallographic temperature factors, or solvation parameters do not always correlate well with the energetic importance of individual residues. Furthermore, the relative contribution of hydrophobicity, surface complementarity, and hydrogen bonding to the energetics of binding and the role of bound water molecules in complex stabilization are not clear. Therefore, structural data combined with comprehensive studies of the energetic contribution of each contact atom are fundamental for the understanding of the chemical basis of macromolecular recognition. Such an approach has been addressed in the well studied interaction of human growth hormone with its receptor, where productive binding was shown to be mediated by a small subset of interfacial residues ("Hot Spot") (*1*, *2*). It was also applied in the energetic analysis of the barnase−barstar interface (*3*) and in the comparison between the energetically important residues involved in the interaction of the antibody (D1.3) and its antigen (HEL) and with its anti-antibody (E5.2) (*4*).

Recently, a high-resolution X-ray crystallographic structure of the complex between the β-lactamase TEM-1[1] and its novel protein inhibitor BLIP has been solved (*5*). This complex was shown to be very stable, with an affinity of 0.6 nM (*6*). Moreover, the crystal structures of the individual proteins are also available (*6*, *7*). Therefore, this system provides an excellent model for studying different aspects of protein−protein interactions. A careful analysis of the interface of the TEM−BLIP complex shows that there are 49 residues which make direct contacts in the complex. Most of these interactions can be divided into two main regions: a concave 'saddle-like' surface of the inhibitor lined by polar, uncharged residues which interacts with a negatively charged protruding loop and short helix (Gln 99−His 112) of TEM-1; and two β-hairpin turns on BLIP, one of which inserts into the positively charged active site of the enzyme. The interactions formed by the two loops of the inhibitor mimic interactions observed with the antibiotic substrate. Asp 49, on one of these loops, is a key residue forming four hydrogen bonds to four conserved residues important in catalysis and

† This research was supported by the Israel Science Foundation founded by the Israel Academy of Sciences and Humanities−Charles H. Revson Foundation (106/97-1) and by a research grant from the Crown endowment fund for immunological research (I327).

* Address correspondence to this author. Fax: 972-8-9344118. E-mail: bcges@wiccmail.weizmann.ac.il.

[1] Abbreviations: BLIP, β-lactamase inhibitor protein; TEM-1, a member of the class A β-lactamase family; SPR, surface plasmon resonance; PADAC, [2-[[*p*-(dimethylamino)phenyl]azo]pyridino]cephalosporin; HBS, Hepes-buffered saline; RU, refractive index unit; PCR, polymerase chain reaction; wt, designates the wild-type protein; Mutant proteins are named with the single-letter code for the wild-type residue, followed by the amino acid position and the single-letter code for the mutation.

10.1021/bi981772z CCC: $18.00
Published on Web 12/10/1998

substrate binding: Ser 130, Lys 234, Ser 235, and Arg 244 [ABL numbering (*8*)]. The position of BLIP-Asp 49 mimics that of the PenG carboxylate in the acyl-enzyme intermediate, where a strong hydrogen bond is formed between the substrate carboxylate and the side chain residues of Arg 244 and Ser 235 (*7*).

Here, we evaluate the kinetics and affinities of binding at various solution conditions of wild-type TEM-1 and BLIP and of alanine substitutions of selected contact residues. We focused our analysis on the multiple interactions between BLIP−Asp 49 and the four TEM-1 residues lining its active site. The interest in this particular site, arises from the analogy between the TEM-BLIP-hairpin interactions and those between TEM-1 and its substrates and its "mechanism-based" inhibitors (*9, 10*). Moreover, this well confined site is located at the edge of the TEM-BLIP interface and therefore, can be treated as a separate binding unit where mutations are not expected to cause changes in the major part of the binding site. Each of the interacting residues was mutated in turn to alanine, and the effect of the mutation on the affinity and on the binding kinetics was determined. Alanine mutations were chosen because alanine eliminates the side chain without altering the main-chain conformation and does not impose extreme steric or electrostatic effects. A better understanding of the energetic contribution of individual contacts in this region to the affinity of TEM-1 and BLIP, may help in the design of novel inhibitors and will hopefully shed some light on the mechanism of protein recognition.

A prerequisite to this analysis is the determination of a precise and fast method for screening affinity and kinetic rate constants. A dissociation constant of a protein complex (K_d) can be obtained either by monitoring the concentration of complex upon titration of one component with a known concentration of the other or by calculating from kinetic data according to $K_d = k_d/k_a$, where k_a and k_d are the association and dissociation rate constants, respectively. The analysis of the interaction between the proteins can be followed either in a homogeneous or in a heterogeneous phase. The former requires specific properties of the interacting proteins such as enzymatic activity, change in fluorescence upon interaction, or different sizes of the interacting molecules. Alternatively, one of the interacting proteins can be labeled. Due to the limitations in the detection of these properties, one is frequently limited by a small range of accessible affinity constants. Label-free solid-phase detection, such as surface plasmon resonance (SPR), is much more attractive for extensive analysis of thermodynamic and kinetic constants (*11, 12*). This method monitors the binding of protein in solution to an immobilized partner. It provides direct access to both association and dissociation rate constants and low sample consumption, and due to its high sensitivity it covers a broad range of measurable affinity constants. Nevertheless, there is increasing evidence that there may be large deviations in the affinities determined from standard binding kinetic measurements using SPR. Some of these problems have been associated to mass transport limitations (*13*), the accessibility of binding sites on the immobilized ligand, heterogeneity of the surface or conformational changes induced due to the immobilization process, interactions within the dextran matrix, and rebinding of protein during the dissociation phase (*14*−*18*). On the other hand, relative parameters can be obtained quite precisely by solid-phase detection, as system-based errors cancel out. We have therefore exploited this technique using a BIAcore instrument for the determination of $\Delta\Delta G_{(mut-wt)}$ and the relative effect mutations have on the kinetic constants of the TEM−BLIP complex.

Here, we establish working conditions and analytical tools to monitor the interaction between TEM-1 and BLIP. We utilize the available structural data combined with protein engineering to understand the contribution of particular residues to the affinity and kinetics of complex formation. To ensure the validity of the data obtained on the BIAcore, affinities and kinetic parameters were measured using fluorescence quench titration, stopped-flow fluorescence (both utilizing tryptophan fluorescence quench), an enzyme inhibition assay (detected by a chromogenic substrate), methods that are based on interactions in a homogeneous phase. We demonstrate that although the values obtained from the SPR analysis are often apparent, the differences in the free energy of interaction, $\Delta\Delta G_{(mut-wt)}$, calculated from the SPR measured data, are the same as those measured by homogeneous phase detection. We show that in the specific site analyzed here, individual residues have a moderate though cooperative contribution to the binding energy of the complex. On the other hand, their effect on the kinetics of association and dissociation is pronounced, especially so for the charged residue. Simple electrostatic rules are used to explain some of this behavior.

MATERIALS AND METHODS

Cloning of the blip Gene. Spores of *S. clavuligerus* were the gift of Y. Aharonowitz from Tel-Aviv University. Genomic DNA from *S. clavuligerus* was isolated according to procedure 4 in (*19*). The DNA was used as a template for the PCR amplification of the *blip* gene (498 bp). Primers containing 23 nucleotides were synthesized according to the coding region of the *blip* gene sequence and its complementary strand (*20*) with flanking *Nde*I (5′) and *Bam*HI (3′) sites, respectively. This fragment was ligated into a pET-9a vector (Promega) which was chosen because it confers a resistance to kanamycin. The plasmids were then transformed into *E. coli* TG1 cells. An efficient transformation was achieved by proper aeration and rotation (>1 h, 37 °C) at the recuperation step. The sequence of *blip* was confirmed by direct sequencing.

Cloning of the TEM-1 Gene. The *bla* gene (861 bp) was amplified by PCR from the plasmid pUC18. Primers containing 23 nucleotides were constructed according to the coding region of the *bla* gene and its complementary strand with flanking *Xba*I (5′) and *Bam*HI (3′) sites, respectively. The amplified fragment was treated as described for the *blip* gene. The pET-9a vector was used here due to the loss of ampicillin resistance of some of the TEM-1 mutants.

Construction of a New Shortened pET-9a Vector for Mutagenesis by PCR. Site-directed mutagenesis of BLIP and TEM-1 was performed by reverse-PCR (*21*). In this method, the entire plasmid is amplified starting from the point of mutation. To increase the efficiency of the amplification using a high fidelity enzyme (PWO, Boehringer Mannheim), we constructed a new plasmid by shortening pET-9a by PCR (using pET-9a with either the inserted *bla* or the *blip* gene as the template). Two 20-mer primers were con-

structed: one from the coding strand starting from *Bgl*II (positions 646−627 of pET-9a) and the other from the complementary strand starting from *Afl*III (positions 2752−2771 of pET-9a). The fragments were purified, phosphorylated, and ligated at room temperature for 1 h. The new plasmid which contains the entire control region and the inserted gene (of either *bla* or *blip*) was transformed into TG1 cells. Protein expression was not impaired by shortening the vector. The new vectors (3096 bp for TEM-1 and 2733 bp for BLIP) were used as templates for all the mutagenesis reactions.

Site-Directed Mutagenesis. For each mutation, two 21-nucleotide primers were constructed. The mutagenic primer, based on the coding strand, had the mutated codon placed at its 5′ end, followed by six codons downstream of the point mutation in the gene sequence. The noncoding primer was composed of the sequence complementary to the seven codons immediately upstream from the site of mutation. Standard PCR conditions were used, with PWO (Boehringer Mannheim) as high fidelity enzyme, 4 mM $MgSO_4$, and the short pET-9a with the appropriate inserted gene as a template. Following phosphorylation of the purified PCR fragment, the blunt ends were ligated and the plasmids were transformed into TG1 cells. The correct single mutations were confirmed by direct sequencing of the gene from both the 5′ and 3′ ends. The efficiency of site-specific mutagenesis is about 90%, with the occurrence of random mutations in 20% of the genes analyzed.

Expression and Purification of Recombinant BLIP and Its Mutants from E. coli. Plasmids harboring the *blip* gene, or its mutant, were transformed to *E. coli* BL21-(pLys S) cells. A 100 mL starter culture was grown overnight at 37 °C in 2×TY medium containing 30 μg/mL kanamycin. This culture was used to inoculate 12 L of medium which contained (w/v) 2% tryptone, 1% yeast extract, 0.25% K_2HPO_4, 0.5% NaCl, 0.1% $MgSO_4$, antifoam and kanamycin (30 μg/mL) at pH 7. The cells were grown in a fermentor at 37 °C. At $A_{600} = 0.6$, protein expression was induced by the addition of 0.2 mM IPTG and growth continued for another 5 h. The pelleted cells were resuspended in lysis buffer (50 mM Tris, pH 8, 100 mM NaCl, 1 mM EDTA, and 50 μg/mL lysozyme), sonicated, and subjected to a French press. Following centrifugation, the inclusion bodies were washed with lysis buffer which did not contain lysozyme and dissolved by stirring in 8 M urea (50−100 mL, 4 °C, for 1 h). The denatured protein solution was refolded by dropwise dilution (10×) into 25 mM Tris, pH 8.4, and then dialyzed 3 times against the same buffer. The protein solution was applied to an ion exchange column (HiTrap Q, Pharmacia) equilibrated with 25 mM Tris, pH 8.4. Following a five column volume wash (4 mL/min), BLIP was eluted with a 0−0.15 M linear gradient of NaCl in Tris buffer over 8 min. BLIP was concentrated with Gyrosep 75 (Intersep) and applied to a Sephadex 75 column (16/26) equilibrated with 50 mM Tris, pH 8.4, and 100 mM NaCl. Pure BLIP eluted after 70 min (1.2 mL/min), yielding 25−50 mg/12 L culture. A single band at 17.5 kDa was observed by SDS−PAGE. The protein was aliquoted, flash-frozen in liquid nitrogen, and stored at −70 °C.

Expression and Purification of TEM-1 and Its Mutants. Plasmids harboring the *bla* gene or its mutants were transformed to *E. coli* BL21(pLys S) cells. A 10 mL starter culture was grown for 6 h on a rotary shaker at 37 °C in 2×TY medium containing 30 μg/mL kanamycin. This culture was used to inoculate 750 mL of 2×TY medium containing either 500 μg/mL ampicillin (for expression of the wild-type protein) or 30 μg/mL kanamycin (for expression of its mutants). At $A_{600} = 0.6$, 0.1 mM IPTG was added and the culture was left overnight. The inclusion bodies (isolated as described for the expression of BLIP) were washed (25 mM Tris, pH 8.4) and dissolved by stirring in 8 M urea (20 mL, 4 °C for 1 h). The denatured protein was refolded by dropwise dilution (10×) into 50 mM Tris, pH 8.0, and then dialyzed against the same buffer. Note that gels of crude expressed TEM-1 yield a doublet with the upper band corresponding to the precursor of β-lactamase which contains a 26 amino acid leader sequence (*22*). The precursor does not refold properly and is separated from the folded protein by centrifugation. The soluble folded protein was then applied to an ion exchange column (HiTrap Q, Pharmacia) equilibrated with 50 mM Tris, pH 8.0. Following a five column volume wash (4 mL/min), TEM-1 eluted with a 0−0.5 M linear gradient of NaCl (in Tris buffer) over 8 min. Fractions containing TEM-1 were concentrated and purified on a gel filtration column as described for BLIP (TEM-1 elutes after 60 min at 1.2 mL/min), yielding 5−20 mg/750 mL culture. A single band at 29 kDa was observed by SDS−PAGE. Both the protein concentration and its activity were determined (as described below). The protein was then aliquoted, flash-frozen in liquid nitrogen, and stored at −70 °C.

Determination of Protein Concentration. Extinction coefficients of $\epsilon_{280} = 28\,460$ for BLIP and $\epsilon_{280} = 28\,960$ for TEM-1 were determined by the method of Gill and von Hippel (*23*). Protein concentrations were determined from the UV absorbance at 280 nm using the appropriate extinction coefficients.

TEM-1 Activity Assay. The activity of TEM-1 was monitored with PADAC (Calbiochem), a colored cephalosporin which undergoes a blue shift upon hydrolysis by the enzyme (*24*). The assay involves monitoring the rate of hydrolysis of the substrate by TEM-1. In a typical experiment, five different solutions of purified TEM-1 (1 nM−0.1 μM, 0.025 M Tris, pH 7.5) were mixed with an equal volume of PADAC solution (10.8 μM in the same buffer), and the decline in A_{572} as a function of time was monitored immediately at 25 °C. The initial rates of hydrolysis were obtained from the slopes of the initial reaction profile. Following the subtraction of the rate of hydrolysis of PADAC in the absence of TEM-1, rates were plotted as a function of TEM-1 concentration. The slope of the linear fit defines the specific activity of TEM-1. In all the experiments described here, the specific activity of TEM-1 was 1.6×10^{-5} s^{-1}.

Enzyme Inhibition Assay. Purified TEM-1 solutions (constant final concentration of 1 nM with BLIP-wt, and 0.1 nM with BLIP-D49A) were mixed with growing concentrations of inhibitor. The mixtures, placed in wells of a disposable multiwell plate, were left on the rocking table (room temperature, 1 h). An aliquot of PADAC solution (to yield a final concentration of 5 μM) was added to each well, and A_{572} was monitored at constant time intervals on a microplate autoreader (with the hydrolysis of PADAC in the absence of TEM-1 as background). The initial rates of hydrolysis were plotted as a function of the BLIP concentration, and

the curves were fitted to eq 1 which expresses the concentration of the complex, [B−T], as a function of K_d (the equilibrium constant for complex dissociation) and the protein molar concentrations [T] and [B] (TEM-1 and BLIP, respectively):

$$[B-T] = \frac{A}{[T]}\left(\frac{-[B]+[T]-K_d}{2} + \sqrt{\frac{([B]+[T]+K_d)^2}{4} - [B][T]}\right) \quad (1)$$

where A is the activity of the noninhibited sample.

Fluorescence Spectroscopy. Fluorescence emission spectra were measured at 25 °C (excitation wavelength of 280 nm, with an excitation and emission bandwidth of 4 nm). Temperature control of the cuvette block was maintained by a thermostated circulating water bath. Samples were scanned from 300 to 400 nm at 1 nm/s. A total of 100 data points were recorded per scan, and 10 scans were averaged. The molar fluorescence coefficients of TEM-1 and BLIP (7800 and 3400, respectively, in 25 mM Tris, pH 7 at 25 °C) were calculated from the slope of the emission (at 340 nm) as a function of protein concentration.

Fluorescence Titration Quench. The emission (at 340 nm) of a 700 μL solution of TEM-1 (0.2 μM) at the appropriate pH was monitored as described above. A total of 20 aliquots of BLIP (2 μL of 7 μM in the same buffer) were titrated to this solution. Following each titration, the solution was mixed and allowed to equilibrate for 4 min before recording the emission. The fluorescence, F, of the mixture of TEM-1 and BLIP at equilibrium is described by the equation (*25*):

$$F = f_T[T] + f_B[B] - f_\Delta 1/2\{([T]+[B]+K_d) - \sqrt{([T]+[B]+K_d)^2 - 4[T][B]}\} \quad (2)$$

where [T] and [B] are the total concentrations of TEM-1 and BLIP, respectively; f_T and f_B are the molar fluorescence of free TEM-1 and BLIP; f_Δ is the molar fluorescence change occurring on complexation, a positive value indicating a net quench; and K_d is the equilibrium constant for complex dissociation. The measured fluorescence was plotted as a function of [B], and the above equation was used to fit the plot. [T] and [B] were treated as independent variables, F was the dependent variable, and f_T, f_B, f_Δ, and K_d were adjustable parameters; the former were optimized by the calculated values above. To measure the pH dependence of the affinity constants, 25 mM buffer solutions were used (MOPS for pH 6.5 and 7.5, Tris for pH 7.5−9).

Determination of Equilibrium Constants Using SPR Detection. The BIAcore system, sensor chips CM5, HBS (10 mM Hepes, 3.4 mM EDTA, 150 mM NaCl, 0.05% surfactant P20, pH 7.4), and the amine coupling kit were obtained from Pharmacia Biosensor AB (Uppsala, Sweden). Prior to any analysis on the BIAcore, the protein samples were centrifuged for 5 min to avoid aggregated material which could interfere with the measurements. The amine coupling kit was used to activate the carboxymethylated dextran surface of the sensor chip. Immobilization was achieved by injecting the desired protein (3 × 20 μL, 5−10 μM in sodium acetate, 20 mM, pH 4.6, 5 μL/min). Residual NHS esters were inactivated with ethanolamine. Between 500 and 3000 RU, depending on the protein, were typically immobilized under these conditions.

Each binding experiment was performed with a constant flow of HBS (or indicated buffer) of 10 μL/min, at 25 °C. Prior to the injection of the analyte, 50 μL of chase solution (containing the wild-type immobilized proteins at a concentration of 1 μM in the same buffer) was injected. This was used to adjust the base line for the direct determination of the dissociation rate constant. Between 50 and 100 μL of analyte (1 μM) was injected over the surface for the association phase, and 250 μL of chase solution was used in the dissociation phase. The surface was regenerated with 20 μL of urea (8 M) followed by an extensive wash of the system and equilibration of the surface with buffer for at least 30 min. Typically, the active fraction of immobilized protein was between 20% and 50%. To estimate the increase in RU resulting from the nonspecific effect of protein on the bulk refractive index, binding of protein to a control surface with no immobilized ligand was also measured (data not shown). This nonspecific signal was nonsignificant for either BLIP or TEM-1 at the concentrations analyzed. Association and dissociation rate constants were determined by analysis of the appropriate regions of the sensogram using the BIAevaluation 2.1 software package (Pharmacia).

Stopped-Flow Measurements. Association rate constants were measured by stopped-flow fluorescence at 25 °C on an Applied Photophysics SX-17MV instrument. Excitation was at 280 nm (slit width 1 mm), and emission was monitored using a cutoff filter of 320 nm. In each experiment, 400 data points were recorded over a 200 s reaction (5 runs were averaged). The fluorescence decrease accompanying the association of TEM-1 to BLIP was monitored under pseudo-first-order conditions where a 5-fold excess of TEM-1 was used. The rates (k), measured for five different concentrations of TEM-1, were calculated by fitting the traces to

$$A = \Delta A e^{-kt} + C \quad (3)$$

where A is the quantity of TEM-1 which is in complex with BLIP at time t, ΔA is the amplitude of the change in A, and C is the offset. The slope of the rates of association, as a function of the molar concentration of TEM-1, defines the association rate constant, k_a.

RESULTS

Recent studies involving BLIP used the purified secreted protein from cultures of *Streptomyces clavuligeurs* (*5, 20*). Here we use, throughout this study, recombinant BLIP overexpressed in *E. coli*. We compare and contrast different methods for the determination of the equilibrium and kinetic constants of the TEM−BLIP complex. These tools are implemented to study the contributions of specific residues to the stability and kinetics of the complex, from which mechanistic considerations can be derived.

Determination of Equilibrium and Kinetic Constants for the Complexation of TEM−BLIP. *(A) Enzyme Inhibition Assay*. The activity of TEM-1 was monitored spectroscopically by the rate of hydrolysis of the colored cephalosporin PADAC (*24*), while binding of BLIP was followed by the inhibition of TEM-1 activity. The initial rates of hydrolysis of the substrate were plotted as a function of BLIP concentration (Figure 1), and the values of K_d were calculated

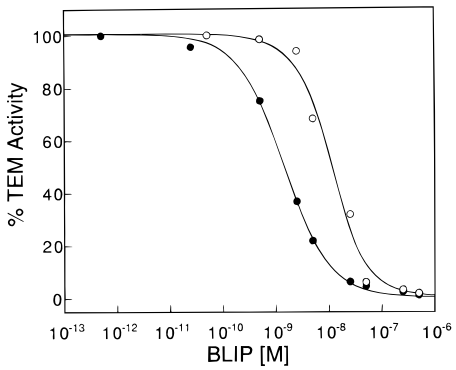

FIGURE 1: Comparison between the affinity of BLIP-wt to TEM-wt (1 nM) (●), and of BLIP-D49A to TEM-wt (0.1 nM) (○), measured by the enzyme inhibition assay (HBS, RT). The activity of TEM-1 was monitored by the rate of hydrolysis of PADAC, followed by the decline in A_{570}. Curves were fit to eq 1, yielding K_d values of 2.3×10^{-9} M for BLIP-wt with TEM-wt and 2.9×10^{-8} M for BLIP-D49A with TEM-wt.

from the fit of the curve to eq 1. The value obtained by this method for the binding affinity of the two wild-type proteins is 0.4 nM (50 mM Tris, pH 7.5, 25 °C). This value is very similar to the affinity of 0.6 nM obtained by a similar assay, using BLIP purified from the secreted media of *S. clavuligerus* (where nitrocefin or imipenem was used as a substrate in 50 mM phosphate buffer, pH 7.0, 30 °C) (*6*). Thus, the activity of the recombinant protein is identical to that of the secreted protein. Due to the sensitivity of the enzymatic activity, one can use very low concentrations of proteins in this assay, thus providing very accurate affinity constants. Note, however, that this assay relies on following the kinetics of TEM-1 activity. Therefore, it is not reliable for measuring affinities of TEM-1 mutants with significantly affected enzymatic activities.

(B) Fluorescence Quench Titration. Fluorescence emission spectra were taken of TEM-1, BLIP, and an equilibrated 1:1 mixture of the two proteins. Figure 2A shows that the fluorescence intensity obtained from the complex is less than the sum of the intensities of the two separate proteins. This observed quench was exploited in order to establish a binding assay for TEM−BLIP. In the titration experiment, a solution of purified TEM-1 was titrated with known concentrations of purified BLIP, and the fluorescence was monitored at a fixed wavelength following an equilibration step (Figure 2B). As the concentration of BLIP approached a 1:1 stoichiometry, a curvature is observed. The size and shape of the curvature depend on the affinity between the two proteins. The curves (obtained from measurements at different pHs, see below) were fitted to eq 2 to derive equilibrium constants (Table 1). Note that the equilibrium constants thus obtained are very sensitive to slight changes in the curve in the breakpoint area which is strongly dependent on the concentration of proteins, especially under conditions of strong affinity. Therefore, for proteins with a high affinity, we approach the limitation of the technique at the protein concentrations needed for detection (this is reflected in a very high standard deviation). Despite this difficulty, the K_d value measured by the enzyme inhibition assay at pH 7.5 is very close to the value measured by this method (Table 1).

(C) Calculation of K_d from Kinetic Data Measured by SPR. TEM-1 or BLIP were covalently immobilized to a carboxymethylated dextran matrix through their primary amine

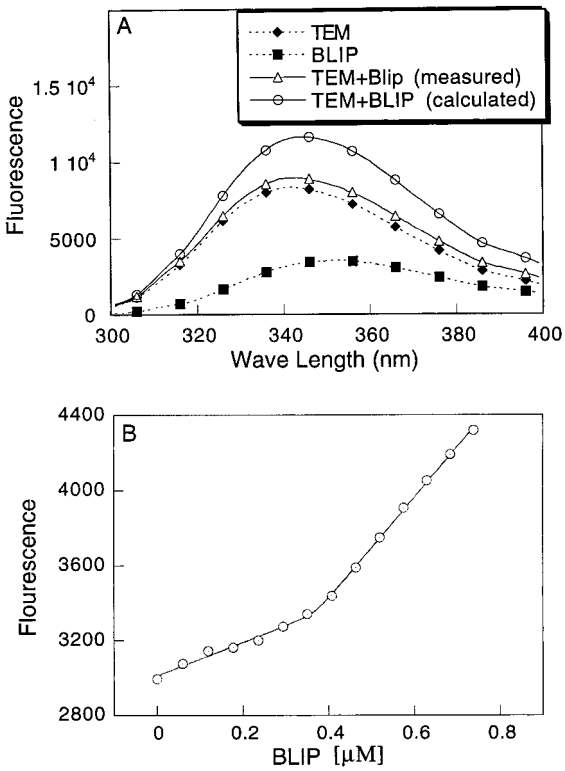

FIGURE 2: (A) Fluorescence emission spectra (measured in arbitrary units) of TEM-1, BLIP, and their 1:1 complex (1.8 μM protein in 50 mM Tris, pH 8.0). The calculated spectrum is the sum of the spectra of TEM-1 and BLIP. (B) A typical curve showing the fluorescence quench observed at 340 nm, upon titration of BLIP to a solution of TEM-1 (0.2 μM in 25 mM Tris, pH 7, at 25 °C). The value of K_d (2.9×10^{-10} M) was obtained by fitting the curve to eq 2.

Table 1: pH Dependence of Kinetic and Equilibrium Constants for Wild-Type TEM-1 and BLIP[a]

	BIA core (TEM-1 immobilized)			stopped-flow fluorescence	fluorescence quench titration	enzyme inhibition assay
pH	k_a ($\times 10^5$) (M^{-1} s^{-1})	k_d ($\times 10^{-4}$) (s^{-1})	k_d/k_a (nM)	k_a ($\times 10^5$) (M^{-1} s^{-1})	K_d (nM)	K_d (nM)
6.5	3.0	3.7	1.2	3.1	2.7	
7.0	2.4	1.6	0.7	2.5	0.3	
7.5	3.1	1.2	0.4	2.4	0.3	0.4
8.0	0.6	2.7	4.5	0.86		
8.5	0.2	6.4	32	0.37	16	
9.0				0.07		

[a] Association (k_a) and dissociation (k_d) rate constants measured by SPR on the BIAcore at 25 °C (25 mM buffer maintained at a constant ionic strength of 0.05 M with NaCl): MOPS, pH 6.5−7.0; Tris, pH 7.5−9) and by stopped-flow fluorescence using the same buffers. Dissociation constants (K_d) were measured directly at the same temperature by fluorescence quench titration (20 mM buffer: PIPES, pH 6.5; Tris, pH 7−8.5) and the enzyme inhibition assay (50 mM Tris, pH 7.5). For SPR data, the average standard deviations are ±7% for k_a, ±5% for k_d, and ±9% for K_d; k_a values measured on the stopped-flow: ±4%; K_d values measured by fluorescence quench titration and the enzyme inhibition assay: ±100% and ±8%, respectively.

groups. Association and dissociation of the soluble partner was followed at real time on the BIAcore by monitoring the change in refractive index associated with its binding or its release from the immobilized ligand. Typical kinetic profiles of the binding of BLIP and of BLIP-D49A to immobilized TEM-1 are shown in Figure 3. To overcome discrepancies in the dissociation rate constants due to rebinding of protein during the dissociation phase, we added protein of the

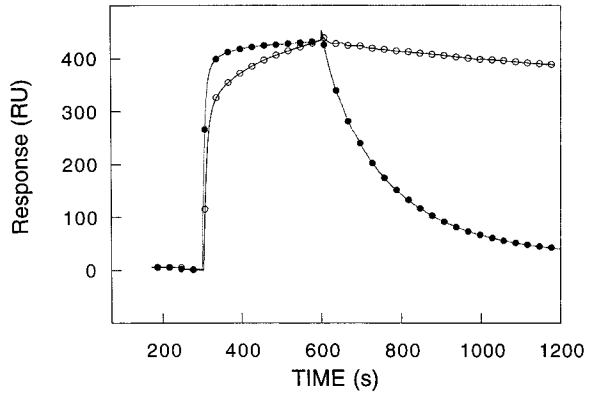

FIGURE 3: Binding of BLIP-wt (○) and BLIP-D49A (●) to TEM-wt measured on a BIAcore (HBS, 25 °C). TEM-1 was immobilized at a level of 2500 RUs. Following the association of 50 μL of 1 μM BLIP, a chase solution containing 1 μM TEM-wt was used during dissociation.

immobilized species to the chase solution. The affinity constants calculated from the kinetic data measured on the BIAcore, with TEM-1 immobilized to the sensor chip, were comparable to those obtained by fluorescence titration, and the enzyme inhibition assay (Table 1), methods that are based on the interaction of the two proteins in a homogeneous phase.

Examination of binding kinetics with BLIP bound to the sensor chip and TEM-1 in solution gave reproducible specific binding. However, the absolute values of the rate constants and of the binding affinities were different from those measured with immobilized TEM-1. Table 2 shows both a slower rate of association and a faster rate of dissociation when the rate constants were measured with BLIP bound to the sensor chip as compared to the rate constants obtained with TEM-1 bound. Thus, one has to be cautious in the determination of absolute kinetic constants using the BIAcore.

While the absolute kinetic constants measured by the BIAcore are erroneous with BLIP bound to the sensor chip, values of the change in free energy for the alanine mutants relative to the wild-type [$\Delta\Delta G_{(\mathrm{mut-wt})}$] did not depend on which protein was immobilized (Table 2). Figure 4 shows a plot of $\Delta\Delta G_{(\mathrm{mut-wt})}$ values obtained from kinetic profiles measured with immobilized TEM-1 versus data obtained with BLIP bound to the sensor chip. It shows a tight correlation with a slope near unity. Furthermore, the value of $\Delta\Delta G_{(\mathrm{mut-wt})}$ measured by the enzyme inhibition assay is comparable to the value obtained by BIAcore (Table 2). Therefore, BIAcore data may be used to determine the value of $\Delta\Delta G_{(\mathrm{mut-wt})}$, which is independent of the method of measurement, since it reflects the net difference in the way in which the mutated protein binds compared to the wild-type.

Characterization of TEM−BLIP Complex Formation. (A) Effect of Solution Conditions. Fluorescence quench titration was employed for the determination of the pH dependence of the dissociation constants of wild-type TEM-1 and BLIP between pH 6.5 and 9. The highest affinity is found at a narrow range of pH values (7−7.5) while at both higher and lower pH values, there is a decrease in affinity. This sharp dependence on pH was confirmed by the dependence of the binding kinetics on pH, measured on the BIAcore and by stopped-flow fluorescence (Table 1). Figure 5 shows that this dependence results from a decrease in the association rate constant above pH 7.5, and an increase of the dissociation rate constant below pH 7 and above pH 7.5. The effect of the buffering agents was evaluated by measuring the association rate constant at pH 7.5 (at a constant ionic strength of 0.05 M maintained with NaCl) in both MOPS and Tris on the stopped-flow machine. The different buffering agents have a small effect on the measured binding kinetics (2.0×10^5 and 2.4×10^5 M^{-1} s^{-1}, respectively). However, it is not large enough to explain the generation of the above profile.

The effect of salt on the binding kinetics of proteins is a measure of the contribution of electrostatic forces to complexation. The association between wild-type BLIP and TEM-1 was measured at different salt concentrations both on the BIAcore (with TEM-1 bound to the sensor chip) and on a stopped-flow instrument. The association rate constant decreases with an increase in the ionic strength of the solution (Figure 6). However, this dependence is fairly low, especially when measured by stopped-flow fluorescence where the association decreased by only 2-fold upon the addition of 0.5 M salt [from 2.5×10^5 to 1.1×10^5 M^{-1} s^{-1}, respectively, while for proteins which are attracted by strong electrostatic forces such as barnase−barstar, a reduction of 2 orders of magnitude was observed (*26*)]. Note that the discrepancy between the BIAcore data and the stopped-flow data is especially pronounced at nonphysiological salt concentrations (see value at 0.02 M, the ionic strength of the solution in the absence of salt, Figure 6). Hence, BIAcore is not the method of choice for measuring association rate constants at extreme salt concentrations. A low dependence on the salt concentration is also observed for the dissociation rate constants (measured on the BIAcore) which increased from 1.2×10^{-4} s^{-1} to 3.5×10^{-4} when going from no added salt to 0.5 M NaCl.

(B) Contributions of Specific Residues. An analysis of the effect of mutations on the rate of association of TEM−BLIP shows that upon removal of positively charged residues on TEM-1, a significant reduction of the relative association rate constant to BLIP is observed (Figure 7A). This is especially pronounced for the double mutant, TEM-K234A, R244A. However, this does not apply for the association of TEM-1 to BLIP-D49A. Here the removal of a negative charge causes an increase in the relative association rate constants. Thus, it seems as though mutations that decrease the negative charge on either one of the proteins increase the association rate constant, whereas mutations which increase the negative charge reduce the association rate constants of the complex formation. Surprisingly, an enhanced association rate constant was also observed for the interaction of BLIP-D49A with TEM-K234A or with TEM-R244A, where both a negative charge and a positive charge were removed from the interface.

While the effect of mutations on the association rate constants depends to a large extent on the charge of the mutated residue, the effect on the dissociation rate constants depends on the disruption of short-range specific interactions and is a measure of the contribution of the mutated residue to the stabilization of the complex. Each of the selected TEM-1 mutations slightly weakens the TEM−BLIP complex, whereas removal of BLIP-Asp 49 (which forms hydrogen bonds with each of the analyzed TEM-1 residues)

Table 2: Kinetic and Equilibrium Constants for Binding TEM-1 and BLIP Mutants[a]

mutated residue		BIAcore (BLIP immobilized)					BIAcore (TEM-1 immobilized)					enzyme inhibition assay		
TEM	BLIP	$k_a(\times10^4)$ ($M^{-1}s^{-1}$)	$k_d(\times10^{-3})$ (s^{-1})	k_d/k_a[b] (nM)	$-\Delta G$[c] (kcal/mol)	$\Delta\Delta G$[d] (kcal/mol)	$k_a(\times10^4)$ ($M^{-1}s^{-1}$)	$k_d(\times10^{-3})$ (s^{-1})	k_d/k_a[b] (nM)	$-\Delta G$[c] (kcal/mol)	$\Delta\Delta G$[d] (kcal/mol)	K_d[b] (nM)	$-\Delta G$[c] (kcal/mol)	$\Delta\Delta G$[d] (kcal/mol)
wt	wt	4.2	0.6	15	10.6		11.9	0.33	2.8	11.6		2.3	11.7	
R244A	wt	1.1	1.6	137	9.3	1.3	2.4	0.67	27.9	10.3	1.4			
S235A	wt	5.7	2.4	43	10.0	0.6	3.4	0.64	18.9	10.5	1.1			
K234A	wt	1.6	1.4	91	9.6	1.1	5.9	0.53	9.0	10.9	0.7			
S130A	wt	3.1	0.9	29	10.2	0.4	0.9	1.10	121	9.4	2.2			
R244A, K234A	wt	0.4	2.1	515	8.5	2.1	20.0	6.5	32.6	10.2	1.5	29	10.25	1.5
wt	D49A	4.6	10.5	227	9.0	1.6	0.9	2.5	2.52	10.6	1.0			
R244A	D49A	4.9	3.3	67	9.8	0.9	19.4	3.8	19.4	10.5	1.15			
S235A	D49A	6.1	7.0	12	9.4	1.2	12.5	2.9	23.5	10.4	1.3			
K234A	D49A	5.5	5.3	98	9.5	1.1	8.0	3.5	44.0	10.0	1.6			
S130A	D49A	4.5	3.8	85	9.6	1.0								
R244A, K234A	D49A	2.8	6.6	241	9.0	1.7								

[a] Binding constants calculated from kinetic data measured on the BIAcore (with either TEM-1 or BLIP immobilized to the sensor chip) are compared to data obtained for TEM-wt using the enzyme inhibition assay (both methods in HBS at 25 °C). The average standard deviations (calculated for data from 2−6 experiments) for data measured with BLIP immobilized are ±12% for k_a, ±15% for k_d, ±20% for k_d/k_a, ±0.1 kcal/mol for ΔG, and ±0.15 kcal/mol for $\Delta\Delta G$; for data measured with TEM-1 immobilized: ±7% for k_a, ±5% for k_d, ±9% for k_d/k_a, ±0.05 kcal/mol for both ΔG and $\Delta\Delta G$; for the enzyme inhibition assay: ±8% for K_d, ±0.05 kcal/mol for ΔG, and ±0.07 kcal/mol for $\Delta\Delta G$. [b] $K_d = k_d/k_a$, the calculated dissociation constant where k_d and k_a are the dissociation and association rate constants, respectively. [c] The free energy of dissociation of the complex, $\Delta G = -RT \ln K_d$. [d] The change in free energy of dissociation for the mutated (mut) relative to the wild-type (wt) protein, $\Delta\Delta G = \Delta G_{mut} - \Delta G_{wt}$.

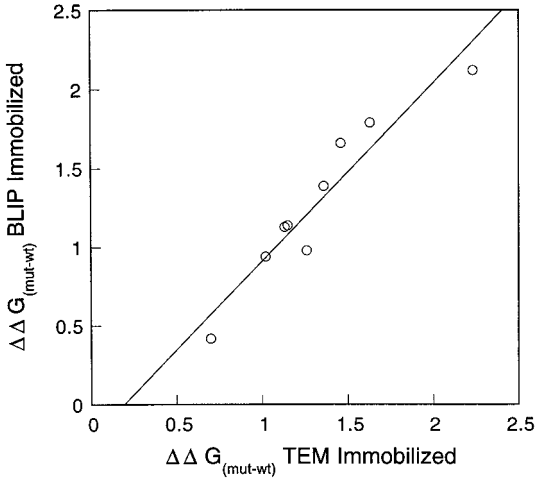

FIGURE 4: Correlation between values of $\Delta\Delta G_{(mut-wt)}$ (kcal/mol) measured on the BIAcore with BLIP bound, and TEM-1 bound to the sensor chip. The slope of the fit is 1.13 ± 0.14. Values are from Table 2.

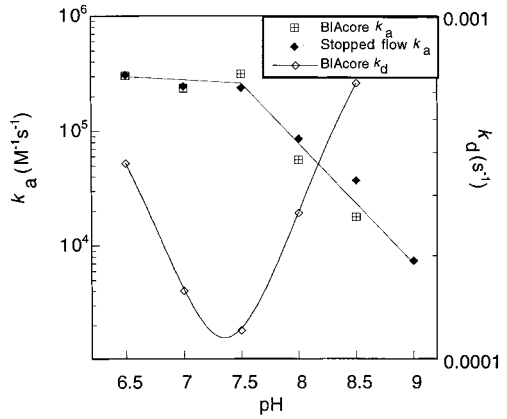

FIGURE 5: pH dependence of the association (k_a) and dissociation (k_d) rate constants of wild-type TEM and BLIP. The values of k_a measured by SPR on the BIAcore are compared to those measured by stopped-flow fluorescence. The drawn lines illustrate the trend of the data. The data are from Table 1.

significantly destabilizes the complex (Figure 7B). The magnitude of the decrease in the binding energy upon truncation of a side chain [$\Delta\Delta G_{(mut-wt)}$] reflects the net effect of the mutation on both association and dissociation, and is an indication of the importance of that residue for complexation. All the chosen mutations destabilize the TEM−BLIP complex [positive $\Delta\Delta G_{(mut-wt)}$ values, Table 2]. However, these values are relatively low in the interaction with BLIP, <1.0 kcal mol^{-1} for the removal of Ser residues and between 1 and 1.5 kcal mol^{-1} upon removal of a positively charged residue on TEM-1. The lower affinity with BLIP results from the reduced association and enhanced dissociation rate constants of the TEM-1 mutants. Elimination of the negative charge on BLIP-D49A weakens the binding interaction with wild-type TEM-1, but its effect over the background of the

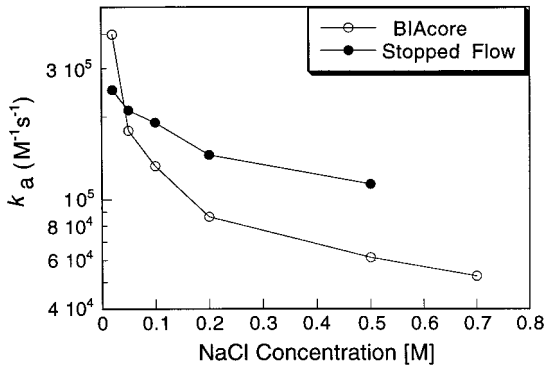

FIGURE 6: Salt concentration dependence of the association rate constant (k_a) of the wild-type TEM−BLIP complex at 25 °C measured on the BIAcore and on the stopped-flow instrument.

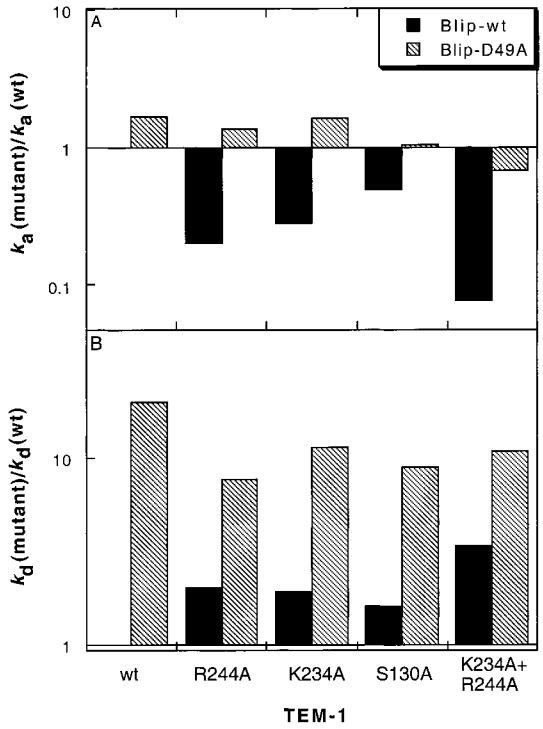

FIGURE 7: Relative change of association (A) and dissociation (B) rate constants for alanine mutants of TEM-1. Black bars are for the interaction with BLIP-wt, and gray bars are for the interaction with BLIP-D49A. The data are taken from Table 2, with TEM-1 immobilized to the sensor chip.

single TEM-1 mutants is relatively low. Thus, the enhanced dissociation rate constants are compensated by the enhanced association rate constants of these proteins. Nevertheless, adding up the $\Delta\Delta G_{(mut-wt)}$ values of all four TEM-1 single mutants gives a value of 3.5 kcal mol^{-1}, which is more than double the loss in free energy upon mutating BLIP-D49A, suggesting the cooperative nature of this binding unit.

DISCUSSION

Here, we describe a kinetic and thermodynamic analysis of the binding of the β-lactamase TEM-1 and its protein inhibitor BLIP. The recombinant protein showed an identical binding affinity to TEM-1 as BLIP purified from the secreted media of *Streptomyces clavuligerus* (0.6 nM) (*6*). We show that this strong affinity is predominantly due to a very stable complex reflected by a slow dissociation rate constant (3×10^{-4} s^{-1}). The association of the two proteins, on the other hand, is comparable to many other protein−protein complexes (2.5×10^5 M^{-1} s^{-1}). However, it is significantly lower than the association rate constants of proteins which are attracted by favorable long-range electrostatic interactions such as barnase−barstar (*26, 27*), hirudin and thrombin (*28*), and ferricytochrome *c* and ferrocytochrome b_5 (*29, 30*) for which association rate constants of over 10^9 M^{-1} s^{-1} (which is close to the diffusion limit) have been detected. Moreover, we observed a relatively low dependence of the association rate constant on the ionic strength of the solution. Hence, electrostatic forces do not seem to contribute to the association of these two proteins.

Here, we show that despite the lack of electrostatic attraction between TEM-1 and BLIP, the association kinetics are highly sensitive to even small changes in the charge of one of the proteins. At ambient pH, both TEM-1 and BLIP carry a net negative charge (−7e and −2e, respectively). Upon mutation of positively charged groups in the binding site of TEM-1, the electronegativity of the protein increases, resulting in a strong decrease of the association rate constants. On the other hand, removal of only one negative charge on BLIP almost neutralizes the protein. Consequently, repulsive forces between the two proteins are removed, and the association rate constants increase.

It has been suggested that the association rate constant is linearly related to the electrostatic energy of interaction of two proteins at an "encounter complex" (*31*). The encounter complex was defined as a state where the two binding sites are aligned, but the proteins remain solvated. To illustrate the effect of electrostatics on the association of TEM-1 and BLIP, we calculated the electrostatic potential at the "encounter complex". Following the calculation, the two proteins were rotated so that their binding surfaces are shown face-on (Figure 8). Figure 8A shows the calculated surface potential felt by the two wild-type proteins. The surface potential of TEM-1 is characterized by an overall negative potential except for the active site pocket, which is strongly positive. The negative potential is especially pronounced in the perturbing loop and helix (Gln 99−His 112) which interacts with a concave polar surface on BLIP. A similar electrostatic description of TEM-1 has been shown before (*32*). The surface potential of BLIP-wt complements that of TEM-1, to some degree, with its strong negative potential located in the vicinity of Asp 49, which interacts with groups lining the positive active site of TEM-1. All-in-all, the surfaces of both proteins are slightly negative, supporting the lack of electrostatic attraction between them. Figure 8B shows the result of the calculated surface potential of the extreme case where the two positive groups, Arg 244 and Lys 234 in the active site of TEM-1, were removed. As a result, the potential of both surfaces becomes strongly negative, resulting in repulsion that is reflected in the slow association rate constant of the double mutant with BLIP. Figure 8C shows the result of the calculated potential of BLIP-D49A and TEM-1. Here, the removal of one negative charge on BLIP eliminated most of the negative potential on the surface of BLIP and caused the perturbing hinge of TEM-1 to become less negative as well. Moreover, the active site of TEM-1 became more positive (note that the electrostatic potentials of the two proteins in the "encounter complex" affect each other). Thus, this mutation removes

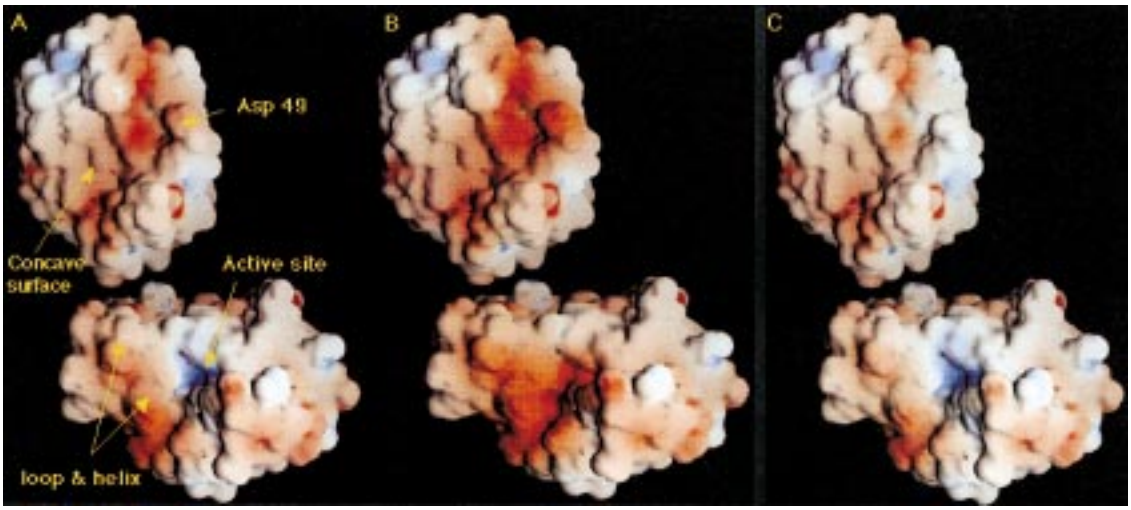

FIGURE 8: Binding surfaces (face-on) of BLIP (upper) and TEM-1 (lower), color-coded according to their electrostatic potential calculated by GRASP (*39*). The calculations were performed at $I = 0.02$ M, with the two proteins in complex, but translated to accommodate a layer of water. Following the calculation, the two proteins were rotated so that their binding surfaces are shown face-on. (A) The two wild-type proteins; (B) BLIP-wt with TEM-K234A, R243A; (C) TEM-wt with BLIP-D49A.

all the repulsive forces between the two proteins, causing the enhanced measured association rate constant. This simple electrostatic calculation can also explain why the TEM-1 mutations K234A and R244A, on a BLIP-D49A background, hardly influence the association rate constant between the two proteins. Together, the calculated surface potentials and the measured association rate constants of the various mutants suggest that although the two wild-type proteins are not strongly attracted by electrostatic forces, mutations of charged residues strongly affect their surface potentials. Consequently, electrostatic forces become predominant factors in the association of the two proteins.

The dependence of the association and dissociation rate constants of the two wild-type proteins on pH may also be explained by simple electrostatic rules. Elevated pK_a's of specific histidine residues located on the binding surface of one of the proteins will result in additional positive charges at ambient pH. A careful analysis of the TEM−BLIP interface reveals that there are four histidine groups on the binding surfaces: His 96 and His 112 on TEM-1 and His 41 and His 148 on BLIP. Charged groups are found in close proximity to each one of them. The pK_a of a free His residue is 6.3, but can be shifted easily by 1 or more pH units by charged groups (*33*). This can explain the higher association rate constants up to pH 7.5, and the drop observed above this pH.

The magnitude of the dissociation rate constant is sensitive to the exact nature of the interacting side chains and relies primarily on the disruption of short-range contacts. Mutation of any one of the TEM-1 residues lining the active site cavity causes the dissociation rate constant to double. However, truncation of BLIP-Asp 49 results in an increase of 1 order of magnitude in the dissociation rate constant of the complex. This is not surprising in light of the fact that Asp 49 interacts with each of the four TEM-1 residues. Hence, mutation of this group alone results in the loss of all four stabilizing residues regardless of which TEM-1 residue has been mutated, if at all. The sum of the $\Delta\Delta G$ values of all four TEM-1 mutants is 3.5 kcal mol^{-1}, which is more than double the loss in free energy upon mutating BLIP-D49A, suggesting the cooperative nature of this binding unit.

We have focused on the energetic analysis of the multiple interactions between BLIP-Asp 49 and the four TEM-1 residues lining its active site, which constitute only one set of interactions that stabilize the TEM−BLIP complex. The values of $\Delta\Delta G_{(mut-wt)}$ measured for all the single mutants in this domain are relatively low (with the highest value of only 1.5 kcal mol^{-1} for BLIP-D49A). This suggests that these residues have relatively low contributions to the complex stabilization. Values of the same order of magnitude have been observed for interacting residues in the binding site of the antibody D1.3 to its antigen (HEL) (*4*), human growth hormone (HGH) with its receptor (*1*, *2*), and barnase with its inhibitor barstar (*3*, *34*). In all these cases, the interacting residues are situated in the periphery and are remote from the center of binding, while $\Delta\Delta G_{(mut-wt)}$ values of residues located at the center of binding sites [so-called "Hot spot" (*2*)] were as high as 6 kcal mol^{-1}. This was independent of whether the central regions form charge contacts (as in barnase−barstar) or hydrophobic contacts (as in HGH−receptor). Peripheral electrostatic interactions were shown to have other roles such as to increase the rate of association (*1*) and to contribute to the specificity of binding by repulsion of nontarget molecules through unfavorable electrostatic or steric interactions (*35*). The peripheral location of this site actually has an advantage for our study, since one can assume that the mutations made here will not affect the rest of the binding site. Moreover, because of its multiple nature, it is ideal for measuring the cooperative effect between interactions within side chains located on two proteins.

We have set two long-term goals for the investigation. One is to understand the cooperative nature of interactions between residues in an interface of a protein complex. The other is to define the nature of the so-called "hot-spot" of an interaction site. Whether or not the functional epitopes of the individual proteins complement each other can easily be approached in the TEM−BLIP interaction, from two interesting angles. One is by mapping the energetically critical residues on different β-lactamases with BLIP, and the other is comparing the interaction of different β-lactamase inhibitors with TEM-1 (as there is a strong analogy between the mode of interaction of BLIP and "mechanism-based"

inhibitors). Another interesting aspect of the TEM−BLIP interaction is the contribution of ordered water in its "functional epitope". The high-resolution crystal structure of the complex indicates the presence of highly ordered water molecules which are predominantly clustered between Gln 99 and His 112 in the enzyme and the polar residues lining the concave side of the inhibitor (*5*). Therefore, this system is ideal for the correlation between solvation and functionality.

Here, we set the foundations for this extensive analysis by establishing working conditions and methods for the rapid and precise determination of binding energies. These were determined by the direct measurement of the equilibrium constant K_d, using the enzyme inhibition assay or fluorescence quench titration (which are independent of the reaction pathway) and by calculating K_d values from k_{off}/k_{on}, which relies on the correct choice of the reaction scheme. As BLIP is a slow tight binding inhibitor of TEM-1, it is reasonable to assume that the process of complexation involves multiple sequential equilibria. A minimalistic reaction scheme for such a reaction involves the formation of at least one encounter complex (A:B) at a rate k_1, which subsequently transforms into the final complex (AB) at a rate k_2, as shown in Scheme 1:

Scheme 1

$$A + B \underset{k_{-1}}{\overset{k_1}{\rightleftharpoons}} A{:}B \underset{k_{-2}}{\overset{k_2}{\rightleftharpoons}} AB$$

As long as (A:B) is in steady-state, thus is not accumulated, K_d can be calculated from k_{off}/k_{on}. This will hold for any number of sequential events. A number of experimental observations support the notion that this is the case for the association of TEM−BLIP. At the concentration range used for this analysis, kinetic profiles measured on the BIAcore do not suggest the accumulation of an intermediate, as only one dissociation phase is observed. [If (A:B) would accumulate, we would expect to see two dissociation phases corresponding to the dissociation of both (A:B) and (AB) to (A+B)]. Furthermore, under pseudo-first-order conditions, a single linear relation between k_{obs} (measured by stopped-flow fluorescence) and concentration was observed. Moreover, for the wild-type proteins and a number of mutants, K_d values obtained directly are equal to those calculated from k_{off}/k_{on}, which is usually an indication that intermediates do not accumulate. Thus, the determination of K_d from k_{off}/k_{on} is justified for this system. We cannot preclude deviations from this scheme at higher protein concentrations, in which case a more complex relationship between rate constants would be needed to derive equilibrium constants.

The use of SPR for the determination of absolute rate constants is controversial, and the determined values have to be treated with suspicion. Deviations from true values may arise from the immobilization process, mass transport effects, fluid dynamics, rebinding, and other limitations arising from the technology itself. Although there is an excellent agreement here between the values of the association rate constants measured by SPR (with TEM-1 bound) and values measured by stopped-flow fluorescence, we caution that this agreement strongly depends on the solution conditions of the experiment (see Figure 6).

The affinities calculated from kinetic data measured on the BIAcore with TEM-1 immobilized to the sensor chip are comparable to those obtained by methods where the proteins are in a homogeneous phase. On the other hand, binding in the reverse orientation, with BLIP bound to the sensor surface and TEM-1 in solution, yielded responses corresponding to lower affinities. This discrepancy may result from repulsion of TEM-1 (which is strongly negative) by the negatively charged dextran layer which supports BLIP. This repulsion can explain the relatively slow association and fast dissociation of TEM-1 to immobilized BLIP, which is not observed when BLIP (which is less negative) is allowed to interact with immobilized TEM-1. Hence, TEM−BLIP complexation provides an excellent example for some of the difficulties which may arise using SPR calculated kinetic data for the determination of equilibrium constants. Nevertheless, the values of $\Delta\Delta G_{(mut-wt)}$ obtained from the BLIP-bound data are the same as those calculated from the TEM-1-bound data and to values obtained by direct determination of K_d. Thus, we can use the BIAcore for the determination of reliable values of $\Delta\Delta G_{(mut-wt)}$ and for the calculation of $\Delta\Delta G_{int}$ by double mutant cycles (*36*). However, when alternative methods for confirming SPR-generated equilibrium constants are not available, it is suggested to use the competitive approach where the binding constants are measured in solution, using the SPR for detection (*14*, *37*, *38*).

ACKNOWLEDGMENT

We thank Tzvia Selzer for her assistance with the GRASP calculations and Dr. Jacob Piehler for his critical reading of the manuscript.

REFERENCES

1. Cunningham, B. C., and Wells, J. A. (1993) *J. Mol. Biol. 234*, 554−563.
2. Clackson, T., and Wells, J. (1995) *Science 267*, 383−386.
3. Schreiber, G., and Fersht, A. R. (1995) *J. Mol. Biol. 248*, 478−486.
4. Dall′Acqua, W., Goldman, E. R., Eisenstein, E., and Maiussa, R. A. (1996) *Biochemistry 35*, 9667−9676.
5. Strynadka, N. C. J., Jensen, S. E., Alzari, P. M., and James, M. N. G. (1996) *Nat. Struct. Biol. 3*, 290−297.
6. Strynadka, N. C. J., Jensen, S. E., Johns, K., Blanchard, H., Page, M., Matagne, A., Frere, J. M., and James, M. N. G. (1994) *Nature 368*, 657−660.
7. Strynadka, N. C. J., Adachi, H., Jensen, S. E., Johns, K., Sielecki, A., Betzel, C., Sutoh, K., and James, M. N. G. (1992) *Nature 359*, 700−705.
8. Ambler, R. P., Coulson, A. F., Frere, J. M., Ghuysen, J. M., Jaurin, B., Jorins, B., Levesque, R., Tiraby, G., and Waley, S. G. (1991) *Biochem. J. 276*, 269−272.
9. Knowles, J. R. (1983) in *Antibiotics VI: modes and mechanisms of microbial growth inhibitors* (Hahn, F. E., Ed.) pp 90−107, Springer-Verlag KG, Berlin.
10. Knowles, J. R. (1985) *Acc. Chem. Res. 18*, 97−104.
11. Johnson, B., Lofas, S., and Lindquist, G. (1991) *Anal. Biochem. 198*, 268−277.
12. Stenberg, E., Pesson, B., Roos, H., and Urbaniczky, C. (1991) *J. Colloid Interface Sci. 143*, 513−526.
13. Karlsson, R., Micharlsson, A., and Mattson, L. (1991) *J. Immunol. Methods 145*, 229−240.
14. Nieba, L., Krebber, A., and Pluckthun, A. (1996) *Anal. Biochem. 234*, 155−165.
15. Schuck, P. (1997) *Curr. Opin. Biotechnol. 8*, 498−502.
16. Schuck, P., and Minton, A. P. (1996) *Trends. Biochem. Sci. 21*, 458−460.

17. O'Shannessy, D. J. (1994) *Curr. Opin. Biotechnol. 5*, 65−71.
18. Edwards, P. R., Gill, A., Pollard-Knight, D. V., Hoare, M., Buckle, P. E., Lowe, P. A., and Leatherbarrow, R. J. (1995) *Anal. Biochem. 231*, 210−217.
19. Hopwood, D. A., Bibb, M. J., Chater, K. F., Kieser, T., Bruton, C. J., Kieser, H. M., Lydiate, D. J., Smith, C. P., Ward, J. M., and Scrempf, H. (1985) *Genetic Manipulation of Steptomyces. A Laboratory Manual*, The John Innes Foundation, Norwich, United Kingdom.
20. Doran, J. L., Leskiw, B. K., Aippersbach S., & Jensen, S. E. (1990) *J. Bacteriol. 172*, 4909−4918.
21. Otzen, D. E., Rheinnecker, M., and Fersht, A. R. (1995) *Biochemistry 34*, 13051−13058.
22. Bowden, G. A., and Georgiou, G. (1990) *J. Biol. Chem. 265*, 16760−16766.
23. Gill, S. C., and von Hippel, P. H. (1989) *Anal. Biochem. 182*, 319−326.
24. Schindler, P., and Huber, G. (1980) in *Enzyme Inhibitors* (Brodbeck, U., Ed.) pp 169−176, Verlag Chemie, Weinheim.
25. Foote, J., and Winter, G. (1992) *J. Mol. Biol. 224*, 487−499.
26. Schreiber, G., and Fersht, A. R. (1996) *Nat. Struct. Biol. 3*, 427−431.
27. Schreiber, G., and Fersht, A. R. (1993) *Biochemistry 32*, 5145−5150.
28. Stone, R. S., Dennis, S., and Hofsteenge, J. (1989) *Biochemistry 28*, 6857−6863.
29. Louie, G. V., and Brayer, G. D. (1990) *J. Mol. Biol. 214*, 527−555.
30. Eltis, L. D., Herbert, R. G., Barker, P. D., Mauk, A. G., and Northrup, S. H. (1991) *Biochemistry 30*, 3663−3674.
31. Vijayakumar, M., Wong, K. Y., Schreiber, G., Fersht, A. R., Szabo, A., and Zhou, H. Z. (1998) *J. Mol. Biol. 278*, 1015−1024.
32. Swaren, P., Maveyraud, L., Guillet, V., Masson, J. M., Mourey, L., and Samama, J. P. (1995) *Structure 3*, 603−613.
33. Loewenthal, R., Sancho, J., Reinikainen, T., and Fersht, A. (1993) *J. Mol. Biol. 232*, 574−583.
34. Schreiber, G., Frisch, C., and Fersht, A. R. (1997) *J. Mol. Biol. 270*, 111−122.
35. Cunningham, B. C., and Wells, J. A. (1991) *Proc. Natl. Acad. Sci. U.S.A. 88*, 3407.
36. Horovitz, A., and Fersht, A. R. (1990) *J. Mol. Biol. 214*, 613−617.
37. O'Shannessy, D. J., and Winzor, D. J. (1996) *Anal. Biochem. 236*, 275−283.
38. Winzor, D. J., and Sawyer, W. H. (1996) *Anal. Biochem. 241*, 180−185.
39. Nicholls, A. (1992) *GRASP, Graphical Representation and Analysis of Surface Properties*, Columbia University, New York.

BI981772Z